Supplementary Information for

CARBON SYSTEM STATE DETERMINES WARMING POTENTIAL OF EMISSIONS

Winkler *et al.*

Corresponding Author: Alexander J. Winkler.
E-mail: alexander.winkler@mpimet.mpg.de *or* awinkler@bgc-jena.mpg.de

This PDF file includes:

Supporting Information Text

S1. Simplifications in the Prevailing Modeling Paradigm of the Coupled Climate Carbon Cycle System

CO_2 emissions translate into a change in global temperature, *i. e.,* TCRE, primarily via three key processes: terrestrial and oceanic CO_2 uptake, the radiative forcing due to atmospheric CO_2, and ocean heat uptake (1, 2). These processes are governed by complex nonlinear mechanisms, but they appear to balance each other, so that TCRE emerges to be a constant in the coupled climate-carbon cycle system as shown by many modeling exercises (1–3). However, the TCRE proportionality and its underlying properties may only hold for the prevailing modeling paradigm and because of the simplifications made in most modeling exercises, as an analysis of simulations of CMIP5 generation Earth system models has already shown (ESMs; 4).

Firstly, the prevailing modeling paradigm, *e. g.,* in the Coupled Climate Carbon Cycle Model Intercomparison Project community (C4MIP; 5, 6), is to force the system with a prescribed atmospheric CO_2 timeline (concentration-driven runs) which suppresses the carbon cycle feedback to atmospheric CO_2 as opposed to emission-driven runs. This paradigm tenaciously persists as it is assumed that the feedback is linear and thus can be reconstructed from concentration-driven runs (7–9). However, Boer *et al.* (10) already demonstrated that the complexity and nonlinearity of the system in fully-coupled emission-driven runs cannot be simplified to a linear behavior.

Secondly, the ESM modeling community focuses on studying TCRE in forcing trajectories that follow a (quasi-)exponentially increasing CO_2 concentration (*e. g.,* 1pctCO2 and RCP8.5 forcing; 6–9). Many key features of TCRE, *e. g.,* the assumption of the linear carbon-cycle feedback, might only hold for this specific scenario. Raupach (11) has analyzed in detail the special case of exponential forcing of the climate carbon cycle and has shown that many aspects of TCRE are scenario specific.

Thirdly, another key shortcoming of TCRE research until today is the focus on atmosphere-ocean coupling and the use of simplified modelling approaches therein, such as analytical models (12) or so-called ESMs of intermediate complexity (EMICs; *e. g.,* in 13–17). The last studies using complex ESMs to investigate pathway dependence in fully-coupled emission-driven runs date back nearly a decade (18–20), and used only a rudimentary representation of the terrestrial biosphere, particularly without consideration of vegetation dynamics. Winkler *et al.* (4), however, suggested that those models from the last generation of complex ESMs (CMIP5 models) with a more comprehensive representation of the terrestrial biosphere reflect strong pathway and state dependence in carbon uptake processes. The C4MIP community also explicitly acknowledges that the lack of accounting for dynamic vegetation in these ESMs could lead to overly conservative estimates of the climate-carbon cycle feedbacks (6).

All three of the shortcomings outlined above, taken together, may be the reason why the climate-carbon cycle feedback connected to vegetation dynamics, and the resulting state dependency of the climate-carbon cycle system has been overlooked to date.

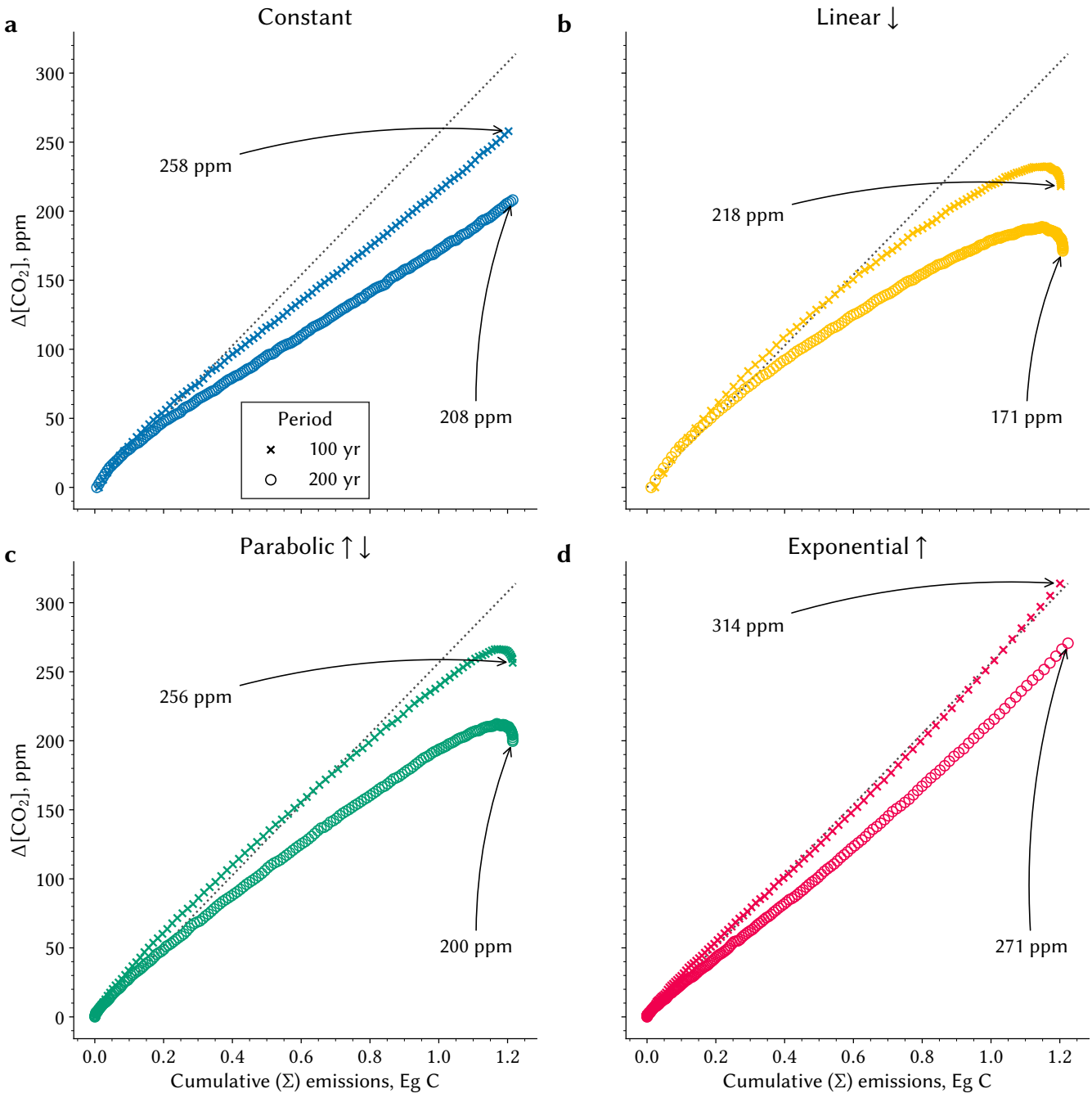

Fig. S1. Change in atmospheric CO_2 concentration across the different pathways and different periods for the same amount of emitted carbon. a–d Relationship between cumulative carbon emissions (*x*-axis) and the change in atmospheric CO_2 concentration ($\Delta[CO_2]$) is shown, where the colors refer to the four different pathways analogous to Figure 1 and the markers refer to the different time periods. The arrows annotate the final $\Delta[CO_2]$ in each model experiment. The dotted black line facilitates comparison between the pathways.

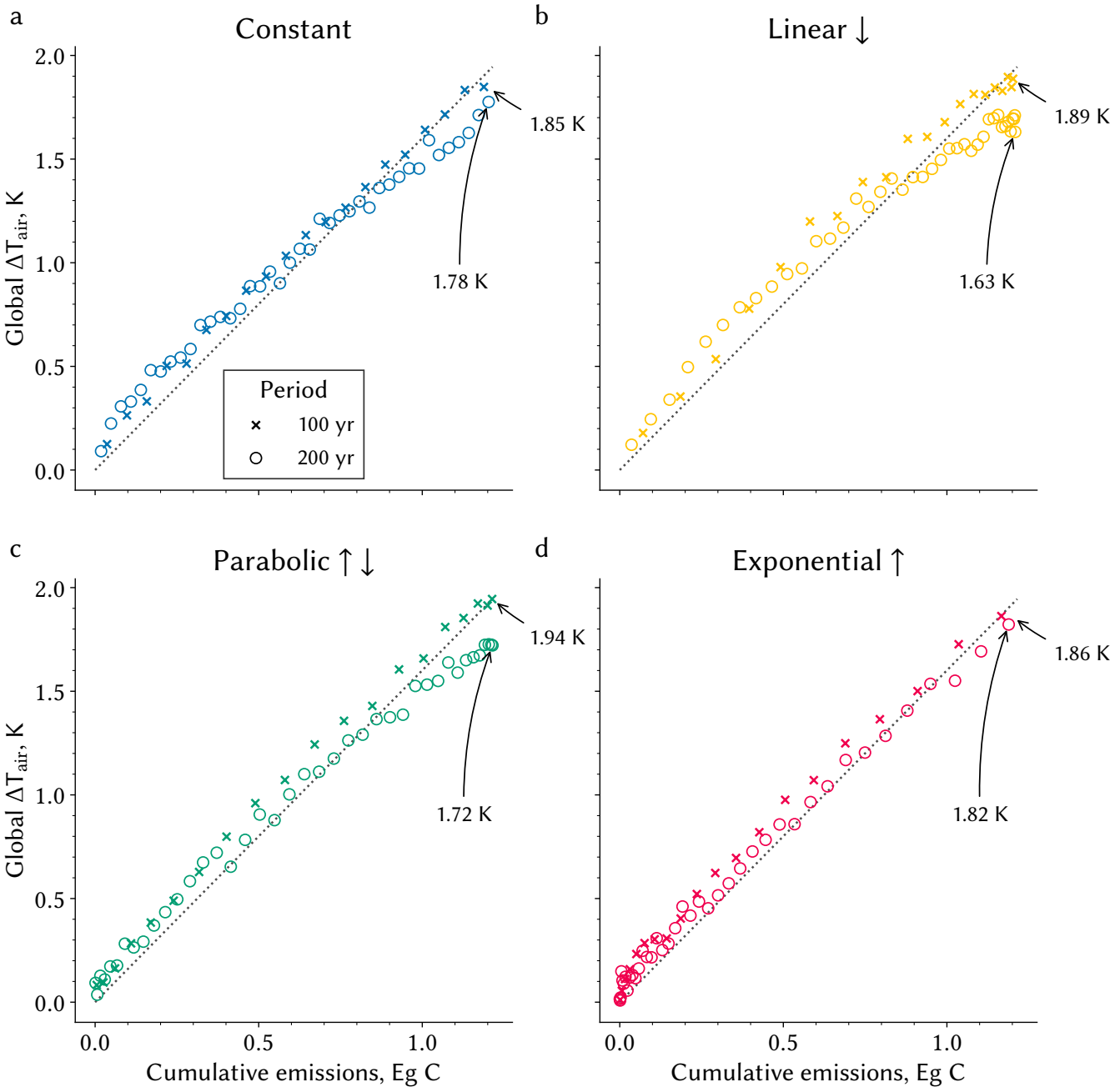

Fig. S2. Change in global mean air temperature across the different pathways and different periods for the same amount of emitted carbon. a–d Relationship between cumulative carbon emissions (*x*-axis) and the change in global mean air temperature (ΔT_{air}) is shown, where the colors refer to the four different pathways analogous to Figure 1 and the markers refer to the different time periods. To reduce inter-annual variability, five-year averages across the three realizations are displayed. The arrows annotate the final ΔT_{air} in each model experiment. The dotted black line facilitates comparison between the pathways.

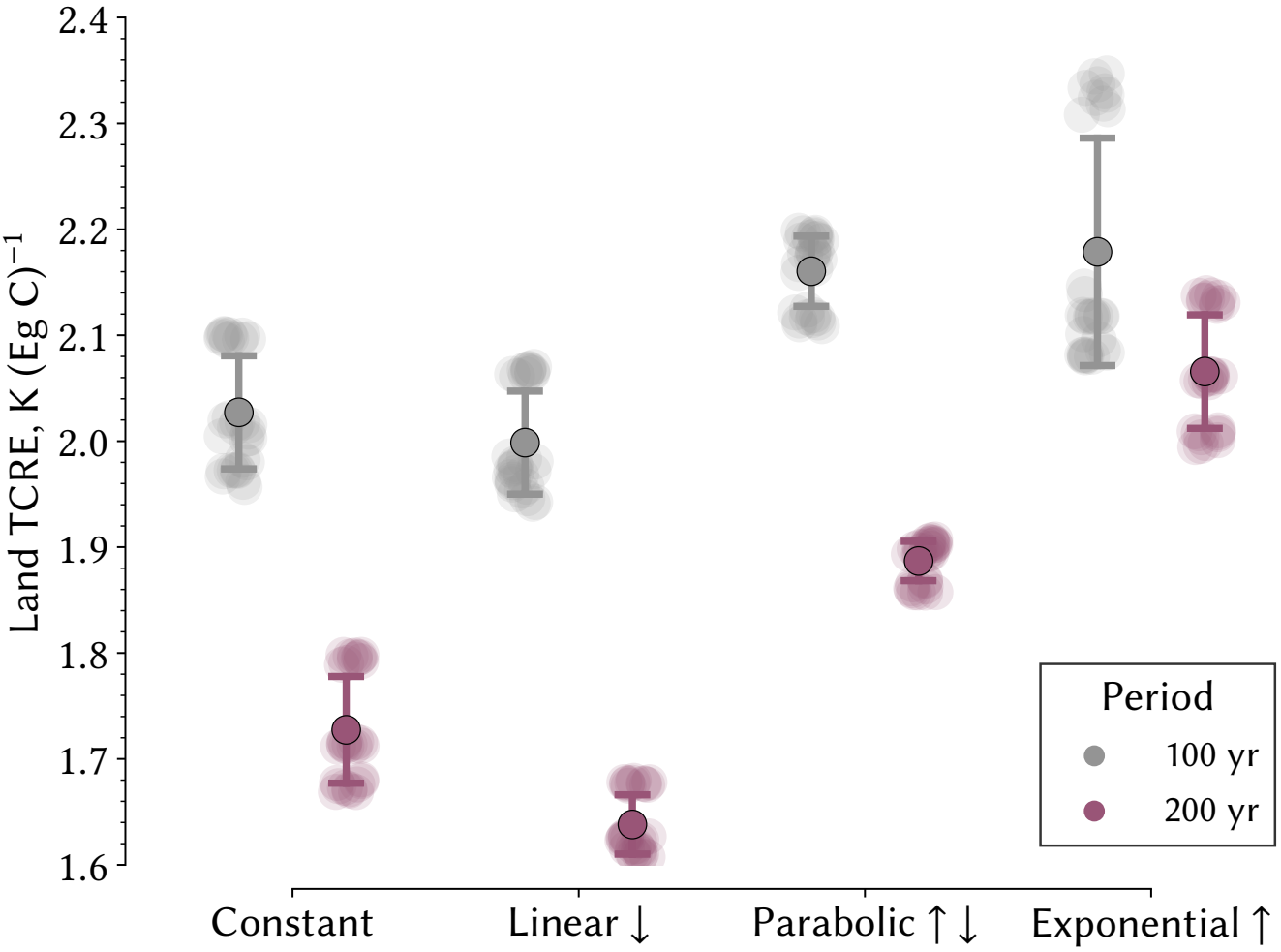

Fig. S3. Pathway dependence of the global carbon cycle response translates into different warming potential of the land for a given emission. Transient Climate Response to Cumulative Emissions (TCRE) for different pathways (*x*-axis) and simulation periods (colors), focusing on the warming of the land surface. Land TCRE is estimated using the conventionally used linear regression method (8). Shaded dots exhibit the spread in the estimates of the final five years when 1.2 Eg C have been emitted as well as among different realizations. Pointplot with whiskers show the mean and standard deviation of the spread.

Table S1. Best-fit values for parameters of the double exponential decay function (Equation 5 in main document) including the standard error (68% confidence) are shown for the CMIP6 ZecMIP multi-model ensemble and the four different emission pathways simulated using MPI-ESM1-2-LR.

Model	η	τ_F	τ_S	C_T^0	C_{OL}^0	R^2
Unit	-	yr	yr	Pg C	Pg C	-
ZecMIP (1000 Pg C)						
ACCESS-ESM1-5	0.13 ± 0.008	20.29 ± 2.01	512.15 ± 29.48	586.78 ± 1.69	418.37	0.996
CESM2	0.34 ± 0.002	28.01 ± 0.22	807.37 ± 12.78	579.10 ± 0.37	425.60	1.000
CanESM5	0.33 ± 0.002	21.74± 0.30	1033.38± 14.78	498.36 ± 1.06	498.02	0.998
GFDL-ESM4	0.31 ± 0.003	26.12 ± 0.58	598.97 ± 11.19	505.69 ± 1.18	496.66	0.998
MIROC-ES2L	0.22 ± 0.003	23.88 ± 0.71	660.19 ± 8.10	516.92 ± 1.49	472.20	0.997
MPI-ESM1-2-LR	0.25 ± 0.003	21.87 ± 0.52	383.24 ± 4.08	536.14 ± 1.17	464.27	0.999
NorESM2-LM	0.35 ± 0.005	27.62 ± 0.42	639.66 ± 28.25	564.94 ± 0.41	439.26	1.000
UKESM1-0-LL	0.17 ± 0.002	30.98 ± 0.76	808.04 ± 7.59	568.75 ± 0.92	426.34	0.998
MPI-ESM1-2-LR Pathways (1200 Pg C)						
Constant	0.28± 0.01	70.92 ± 2.58	1152.43 ± 54.47	434.98 ± 0.72	773.10	0.998
Linear ↓	0.24 ± 0.01	80.40 ± 3.96	1694.86 ± 127.91	364.70 ± 0.59	843.32	0.997
Parabolic ↑↓	0.31 ± 0.01	92.89 ± 4.05	1700.77 ± 163.26	417.87 ± 0.58	793.13	0.998
Exponential ↑	0.35 ± 0.01	61.72 ± 1.67	943.89 ± 36.29	559.11 ± 1.04	652.48	0.998

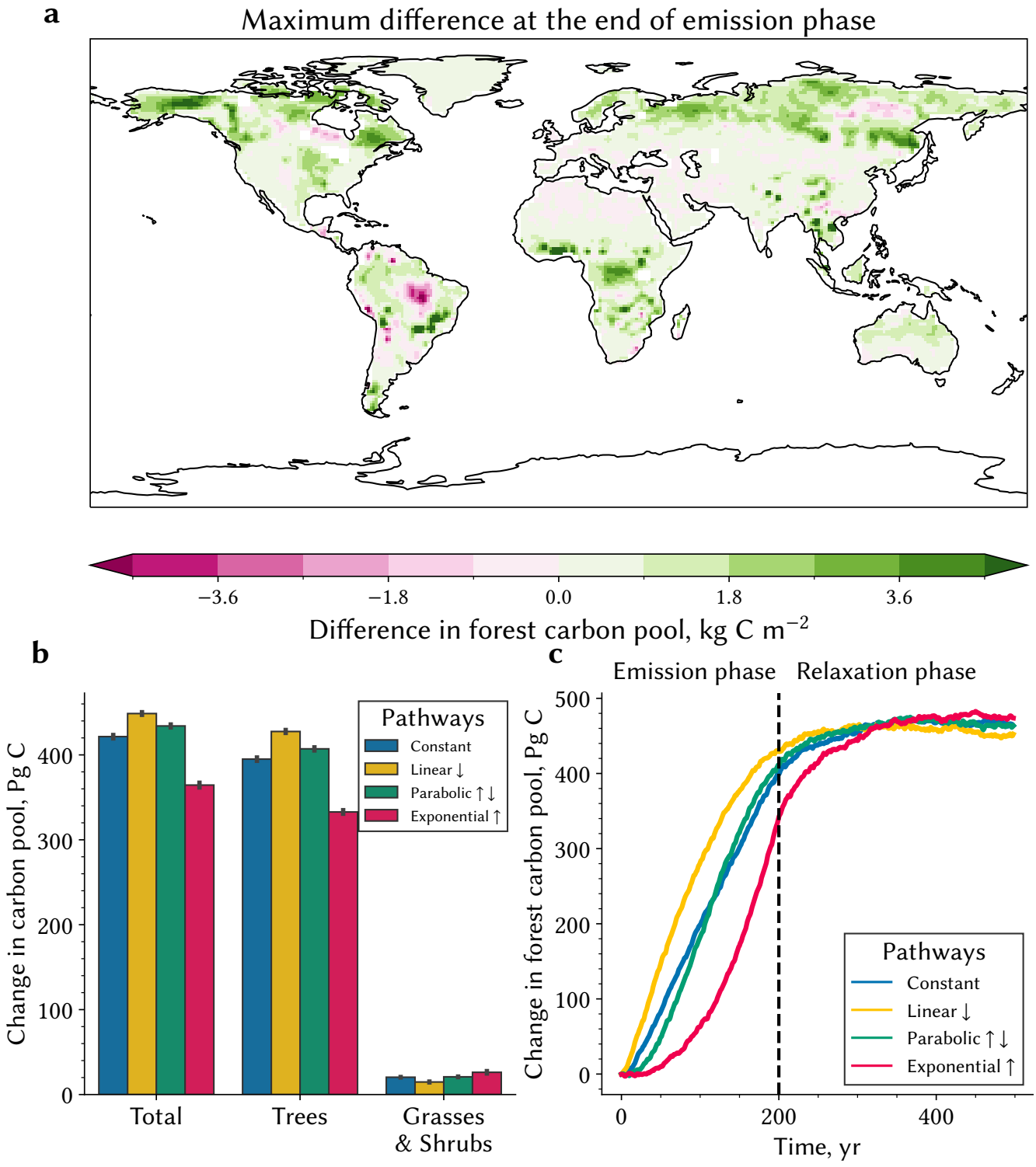

Fig. S4. Vegetation dynamics explain the pathway dependence in the terrestrial carbon cycle. a Global map of the difference in the total forest carbon pool between the L and E pathways (yellow and red in b and c, respectively) at the end of the emission phase, calculated with MPI-ESM1-2-LR in the 200-year runs. **b** Change in carbon pool for forest, grass- and shrublands, and total vegetation for the different emission pathways. The whiskers represent the uncertainty between the different realizations. **c** Change of forest carbon pool across the four pathways as a function of time for both the emission and relaxation phases.

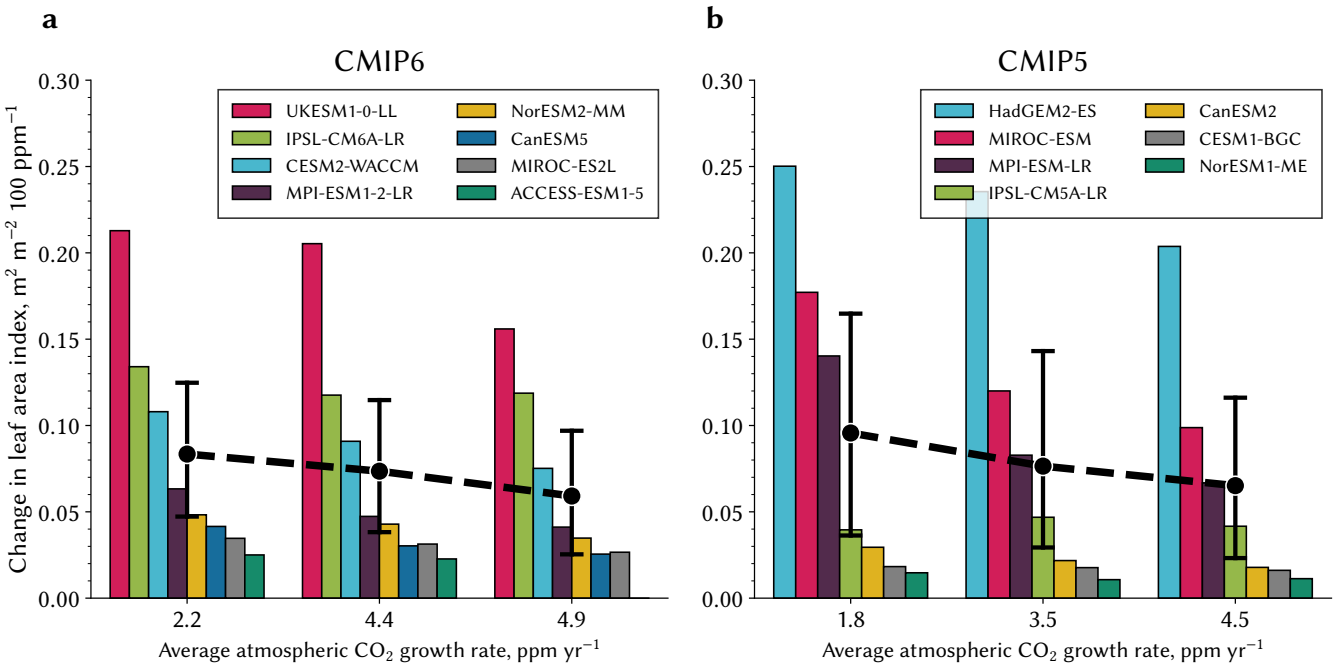

Fig. S5. Leaf area sensitivity to different CO_2 growth rates in CMIP ensembles a Change in leaf area index at latitudes above 60 ° N per a 100 ppm change in atmospheric CO_2 across three different future scenarios in CMIP6 reflecting different CO_2 growth rates (*x*-axis). The black dot refers to the multi-model mean value for each growth rate, where the whiskers represent the standard deviation. **b** as in c but for CMIP5.

Table S2. Best-fit values for parameters of the double exponential decay function (Equation 5 in main document) are shown, where η is sampled from the parameter space determined in Table S1. The uncertainty estimate refers to one standard deviation of the individual parameter estimates between samples. Results are shown for the CMIP6 ZecMIP multi-model ensemble and the four different emission pathways simulated using MPI-ESM1-2-LR.

Model	η	τ_F	τ_S	C_T^0	C_{OL}^0	R^2
Unit	-	yr	yr	Pg C	Pg C	-
ZecMIP (1000 Pg C)						
ACCESS-ESM1-5	[0.13 – 0.35]	20.52 ± 3.66	519.06 ± 63.81	586.29 ± 0.82	418.37	0.995 ± 0.000
CESM2	[0.13 – 0.35]	28.40 ± 5.39	1037.60 ± 622.43	577.74 ± 2.53	425.60	0.999 ± 0.001
CanESM5	[0.13 – 0.35]	23.33 ± 3.52	1269.50 ± 628.47	493.79 ± 11.17	498.02	0.992 ± 0.005
GFDL-ESM4	[0.13 – 0.35]	27.47 ± 5.50	647.11 ± 168.05	502.13 ± 3.07	496.66	0.997 ± 0.001
MIROC-ES2L	[0.13 – 0.35]	26.22 ± 5.03	689.80 ± 95.04	512.74 ± 5.50	472.20	0.995 ± 0.001
MPI-ESM1-2-LR	[0.13 – 0.35]	23.17 ± 4.37	394.77 ± 50.94	532.64 ± 3.23	464.27	0.998 ± 0.001
NorESM2-LM	[0.13 – 0.35]	27.57 ± 4.25	830.64 ± 521.07	564.98 ± 2.09	439.26	1.000 ± 0.000
UKESM1-0-LL	[0.13 – 0.35]	33.26 ± 6.19	831.35 ± 92.55	565.85 ± 3.03	426.34	0.998 ± 0.001
MPI-ESM1-2-LR Pathways (1200 Pg C)						
Constant	[0.24 – 0.35]	75.53 ± 10.00	1318.27 ± 291.27	434.38 ± 1.27	773.10	0.998 ± 0.000
Linear ↓	[0.24 – 0.35]	101.18 ± 11.81	3483.91 ± 1738.02	363.31 ± 0.74	843.32	0.997 ± 0.000
Parabolic ↑↓	[0.24 – 0.35]	90.62 ± 10.56	1708.37 ± 438.07	418.08 ± 0.84	793.13	0.998 ± 0.000
Exponential ↑	[0.24 – 0.35]	50.18 ± 7.10	742.98 ± 111.07	561.10 ± 0.97	652.48	0.997 ± 0.001

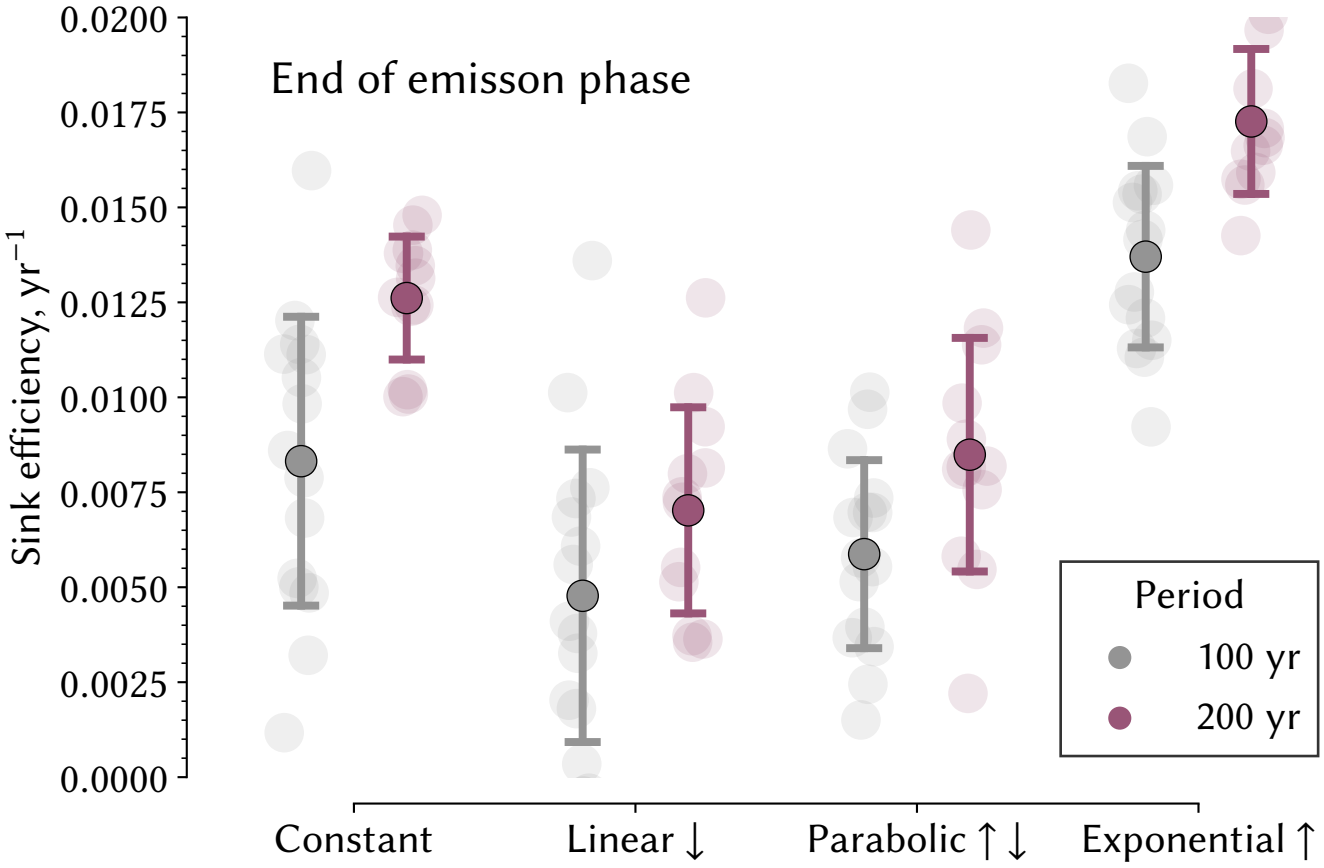

Fig. S6. Sink efficiency differs across pathways after emission cessation of the same amount of carbon. Sink efficiency for different pathways (x-axis) and simulation periods (colors) at the end of the emission phase. Shaded dots exhibit the spread in the estimates of the final five years when 1.2 Eg C have been emitted as well as among different realizations. Pointplot with whiskers show the mean and standard deviation of the spread.

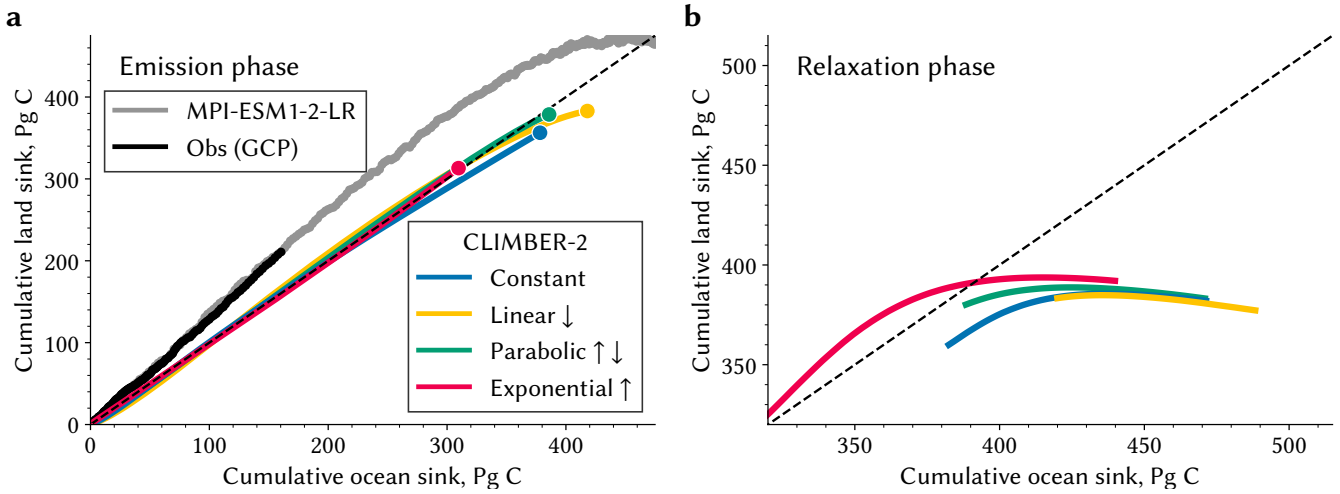

Fig. S7. Partitioning of emissions into land and oceans sinks across the pathways in the EMIC CLIMBER-2 a Cumulative land and ocean sinks are juxtaposed across all pathways. The markers denote the final state at the end of the emission phase of 1.2 Eg C. The dashed line indicates equal magnitude of cumulative land and ocean sinks. The gray and black lines refer to the relationships inferred from MPI-ESM1.2-LR simulations and GCP estimates, respectively. **b** As in a, but for relaxation phase. The Climate-Biosphere model (version 2) CLIMBER-2 is an Earth System Model of Intermediate Complexity (EMIC) and consists of a statistical-dynamical atmosphere component ($51^\circ \times 10^\circ$ spatial resolution), a 2D ocean component with three zonally averaged basins, and a land component including dynamic vegetation (21). The same model version of CLIMBER-2 is used, which was also used for the ZecMIP runs (22).

References

1. JM Gregory, CD Jones, P Cadule, P Friedlingstein, Quantifying Carbon Cycle Feedbacks. *J. Clim.* **22**, 5232–5250 (2009).
2. JG Canadell, et al., Global Carbon and other Biogeochemical Cycles and Feedbacks in *Climate Change 2021: The Physical Science Basis. Contribution of Working Group I to the Sixth Assessment Report of the Intergovernmental Panel on Climate Change*. (Cambridge University Press, Cambridge, United Kingdom and New York, NY, USA), (2021).
3. HD Matthews, NP Gillett, PA Stott, K Zickfeld, The proportionality of global warming to cumulative carbon emissions. *Nature* **459**, 829–832 (2009).
4. AJ Winkler, RB Myneni, V Brovkin, Investigating the applicability of emergent constraints. *Earth Syst. Dyn.* **10**, 501–523 (2019).
5. VK Arora, et al., Carbon–Concentration and Carbon–Climate Feedbacks in CMIP5 Earth System Models. *J. Clim.* **26**, 5289–5314 (2013).
6. VK Arora, et al., Carbon–concentration and carbon–climate feedbacks in CMIP6 models and their comparison to CMIP5 models. *Biogeosciences* **17**, 4173–4222 (2020).
7. P Friedlingstein, et al., Uncertainties in CMIP5 Climate Projections due to Carbon Cycle Feedbacks. *J. Clim.* **27**, 511–526 (2013).
8. RG Williams, P Ceppi, A Katavouta, Controls of the transient climate response to emissions by physical feedbacks, heat uptake and carbon cycling. *Environ. Res. Lett.* **15**, 0940c1 (2020).
9. CD Jones, P Friedlingstein, Quantifying process-level uncertainty contributions to TCRE and carbon budgets for meeting Paris Agreement climate targets. *Environ. Res. Lett.* **15**, 074019 (2020).
10. GJ Boer, VK Arora, Feedbacks in Emission-Driven and Concentration-Driven Global Carbon Budgets. *J. Clim.* **26**, 3326–3341 (2013).
11. MR Raupach, The exponential eigenmodes of the carbon-climate system, and their implications for ratios of responses to forcings. *Earth Syst. Dyn.* **4**, 31–49 (2013).
12. AH MacDougall, The Transient Response to Cumulative CO_2 Emissions: A Review. *Curr. Clim. Chang. Reports* **2**, 39–47 (2016).
13. T Herrington, K Zickfeld, Path independence of climate and carbon cycle response over a broad range of cumulative carbon emissions. *Earth Syst. Dyn.* **5**, 409–422 (2014).
14. P Goodwin, RG Williams, A Ridgwell, Sensitivity of climate to cumulative carbon emissions due to compensation of ocean heat and carbon uptake. *Nat. Geosci.* **8**, 29–34 (2015).
15. M Steinacher, F Joos, Transient Earth system responses to cumulative carbon dioxide emissions: Linearities, uncertainties, and probabilities in an observation-constrained model ensemble. *Biogeosciences* **13**, 1071–1103 (2016).
16. AH MacDougall, The oceanic origin of path-independent carbon budgets. *Sci. Reports* **7**, 10373 (2017).
17. AK Seshadri, Origin of path independence between cumulative CO_2 emissions and global warming. *Clim. Dyn.* **49**, 3383–3401 (2017).
18. K Zickfeld, VK Arora, NP Gillett, Is the climate response to CO_2 emissions path dependent? *Geophys. Res. Lett.* **39** (2012).
19. D Nohara, Y Yoshida, K Misumi, M Ohba, Dependency of climate change and carbon cycle on CO2 emission pathways. *Environ. Res. Lett.* **8**, 014047 (2013).
20. JP Krasting, JP Dunne, E Shevliakova, RJ Stouffer, Trajectory sensitivity of the transient climate response to cumulative carbon emissions. *Geophys. Res. Lett.* **41**, 2520–2527 (2014).
21. V Brovkin, et al., Carbon cycle, vegetation, and climate dynamics in the Holocene: Experiments with the CLIMBER-2 model. *Glob. Biogeochem. Cycles* **16**, 86–1–86–20 (2002).
22. AH MacDougall, et al., Is there warming in the pipeline? A multi-model analysis of the Zero Emissions Commitment from CO_2. *Biogeosciences* **17**, 2987–3016 (2020).